American Journal of Engineering Research (AJER) ***2017***
American Journal of Engineering Research (AJER)
e-ISSN: 2320-0847 p-ISSN : 2320-0936
Volume-6, Issue-12, pp-439-447
www.ajer.org
Research Paper Open Access

Ab initio study of the electronic band structure and phonon dispersion spectra of Silicon disulphide (SiP_2) and Silicon diarsenide ($SiAs_2$)

Omehe N. N.[1], Otete I.[2]
[1](*Department of Physics, Federal University, Otuoke, Nigeria)*
[2](*Department of Physics, Federal University, Otuoke, Nigeria)*
Corresponding Author: Omehe N. N

Abstract: *The electronic band structure and vibrational properties of SiP_2 and $SiAs_2$ have been calculated within the framework of the density functional theory (DFT) and the density perturbation functional theory (DPFT) respectively. For exchange and correlation, the local density approximation was used. The structural optimization results agree well with experiment. The calculation showed that both materials are semi-metals with negative band gap values of -0.91 eV and -1.14 eV for SiP_2 and $SiAs_2$ respectively. The highest frequency mode was observed to be one of the triply degenerated mode T_g with vibrational frequency value of 487 cm^{-1} for SiP_2 and 442 cm^{-1} for $SiAs_2$.*

Keywords: *SiP_2 and $SiAs_2$, Electronic band structure, Phonon curve of SiP_2 and $SiAs_2$, Vibrational properties of SiP_2, Vibrational properties of $SiAs_2$.*

Date of Submission: 14-12-2017 Date of acceptance: 03-01-2017

I. INTRODUCTION

SiP_2 and $SiAs_2$ crystallizes in the pyrite structure. The pyrite structure is formed by compounds of the form MX_2, MXY or MY_2 where M is usuallu a transition metal and X, Y stand for 6B or 5B elements of which SiP_2 and $SiAs_2$ are typical [1]. The pyrite structure of SiP_2 and $SiAs_2$ is a network of Silicon octahedral, each of which is a pair of Phosphorus (P) or Arsenic (As) atoms inside [2]. The silicon (Si) atoms have a sixfold coordination with six P or As atoms arranged as a regular octahedron [2].

The materials under investigation have attracted the attention of researchers, both experimentally and theoretically. The earliest experimental study of the silicon-Arsenic system was that of Klemm and Pirscher in 1941. They observed and reported two intermediate phases of the silicon-Arsenic system from the analysis of their phases equilibrium data [3]. These materials, and in general, the transition metal dichalcogenides (TMDCs) are novel materials with technological application in emerging electrodes materials for water electrolysis and batteries [4].

Osugi et al [5] in their work, subjected silicon and phosphorus to high temperature of about 1100-1500 ◦ C and pressure of about 20-40 kbar, the result was SiP_2 cubic compound with pyrite structure as revealed by their X-ray powder analysis (pattern).Wadsten [1] obtained SiP_2 by heating the constituent of the material (silicon powder and red phosphorus) in a silica tube to a temperature of 600 ◦C ,some what lesser than that of Osugi et al. His guninier powder pattern was in agreement with Osugi et al. Donohue et al [6], described the preparation and properties of pyrite-type SiP_2 and $SiAs_2$. They prepared SiP_2 by halogen transport while $SiAs_2$ was prepared by high pressure synthesis. The resulting structure of the materials showed agreement with previously obtained results.

Chattopadhyay and schnering also studied the structure of SiP_2 using X-ray and neutron diffraction. Again, their results agreed well with the results of previous studies [7]. Vogt et al [8] worked on the raman spectra of FeS_2, MnS_2 and SiP_2. They reported that the modes Ag, Eg, T^1_g, T^2_g and T^3_g for SiP_2 had frequencies 461 cm^{-1}, 353 cm^{-1}, 319 cm^{-1}, 337 cm^{-1} and 485 cm^{-1} respectively.

Theoretically, a number of researchers have taken interest in SiP_2. Bachhuber et al [9] in their first principle calculations on structure, bonding and vibrational frequencies of SiP_2, using LDA, GGA, B3LYP and HF

functional, reported a semimetallic nature for SiP_2 except for the Hartree-Fock (HF) method which gave a band gap value of 4.8 eV. They also reported various frequencies for some selected raman modes from the calculations of the different functional they used.

SiP_2 and $SiAs_2$ materials have been known for sometime now, to the best of our knowledge, few theoretical work have been carried out on them, especially on $SiAs_2$ where literature were scarcely available. To the best of our knowledge, the full phonon dispersion curves for these materials have not been reported. So, in this study, the electronic band structure and phonon dispersion curves for SiP_2 and $SiAs_2$ have been investigated.

II. COMPUTATIONAL DETAILS

The structure used in the computation is shown in figure 1. SiP_2 and $SiAs_2$ crystallize in a cubic structure. It has a space group number of 205, that is the space group of Pa3 [1-6]. In this work, the structural optimization, electronic band structure and phonon vibrational frequencies were computed for the materials under investigation. The structural optimization was computed in two stages. Firstly, the atomic coordinates with silicon (Si) at the 4a and phosphorus P (As) at the 8c Wyckoff's atomic positions were relaxed. The relaxed atomic positions were then used in the lattice parameter optimization. Both the relaxed atomic coordinates and the lattice parameters were allowed to evolve in this second stage. Fig 1 shows the structure used in the computation. The experiment value of the lattice parameter of 5.705 Å [1-6] was used as the starting point. The force tolerance for both stages of the optimizationwas 10^{-3}br/atom (bohr/atom). Table 1 shows the result of the optimization together with the experimental data.

There are four formula unit contained in a unit cell, this brings the number of atomic postions used in the computation to 12. The pseudopotential method was used in this study, utilizing the norn-conserving [10] pseudopotential within the frame work of density functional theory as implemented in the Abinit package [11, 12]. For exchange and correlation, the parametrization of Perdew and Zunger [13] was used. The plane waves were generated by a kinetic energy cutoff of 540 eV. A 128 k-point mesh generated by a 4x4x4 shifted grid. The self consistency calculation tolerance on energy was $1.0x10^{-10}$. While for the response function computation, the kinetic energy cutoff of 165 eV was used for plane waves generation. The wave vectors (q-point) used were generated by an unshifted 4x4x4 grid. The phonon calculation was performed within the frame work of the self consistency density functional perturbation theory (DFPT) [14, 15, 16]. The generated q-points gave a good phonon dispersion curve.

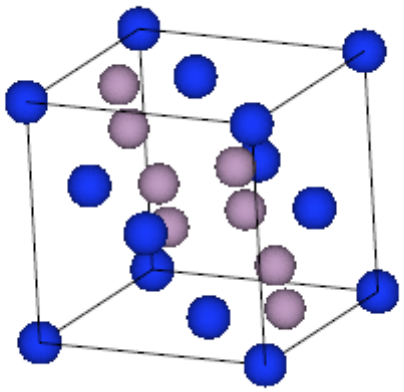

Figure 1: The structure used for the computation. The blue balls represent the silicon (Si) atoms while the grey balls represent the phosphorus (P) or Arsenic (As) atoms.

Table 1: Optimization result and experimental data.

	This study	Exp [17]	Exp [1]	Exp [2]	Calculated [9]
Lattice Parameter a(Å) for SiP_2	5.7026		5.707 (at 293K) X-ray	5.705	
			5.706 (at 293K) Neutron		
			5.681 (at 60K) Neutron		
SiP_2 bond lengths (Å) Si-Si	4.0324		4.035 at 293K	4.03	
Si-P	2.41		2.398	2.36	2.375 (LDA)
P-P	2.04		2.16	2.16	2.155 (LDA)

Lattice Parameter $SiAs_2$ in (Å)	6.1027	6.104			
Bond lengths in (Å) Si-Si Si-As As-As	 4.32 2.59 2.14				

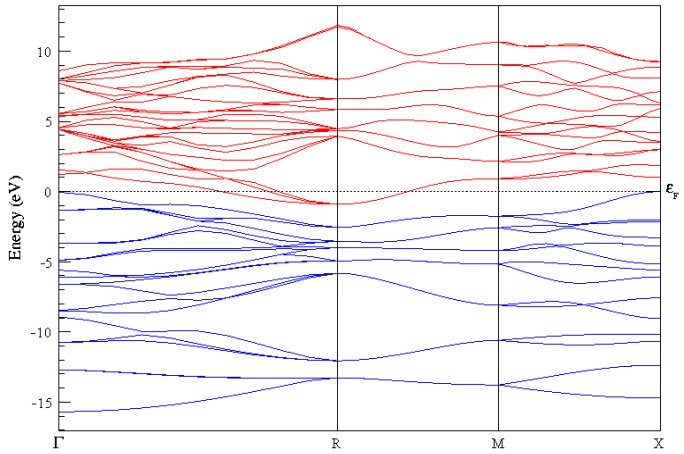

Figure 2: The electronic band structure of SiP_2, whereϵ_F represents the Fermi energy

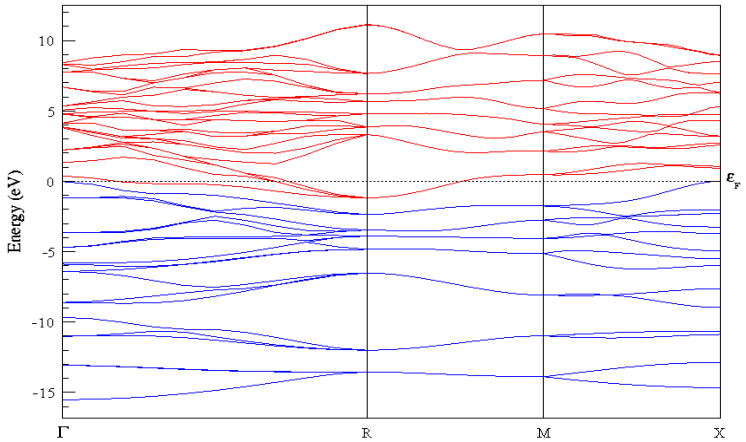

Figure 3: The band structure of $SiAs_2$, whereϵ_F represents the Fermi energy

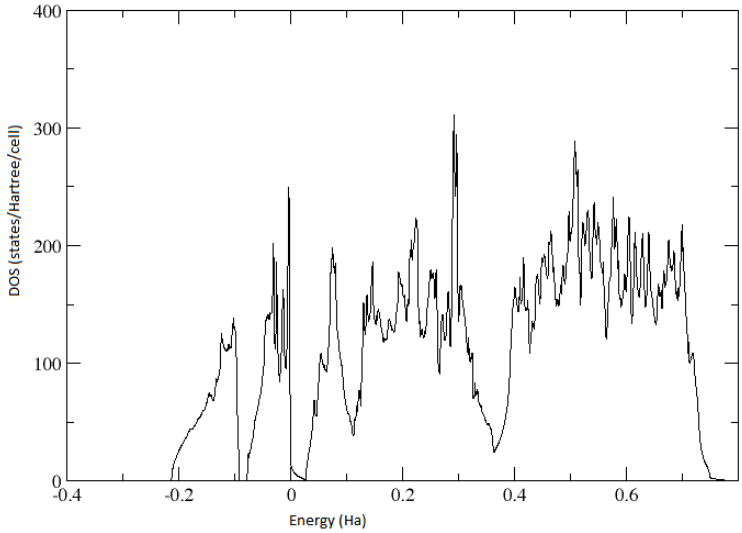

Figure 4: The total density of states DOS for SiP_2. The Fermi energy is at 0.36 Ha.

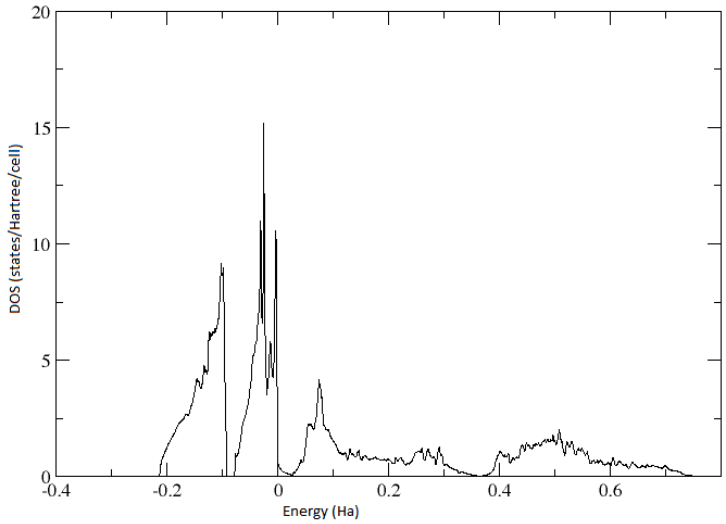

Figure 5: The P-3s orbital contribution to the DOS.

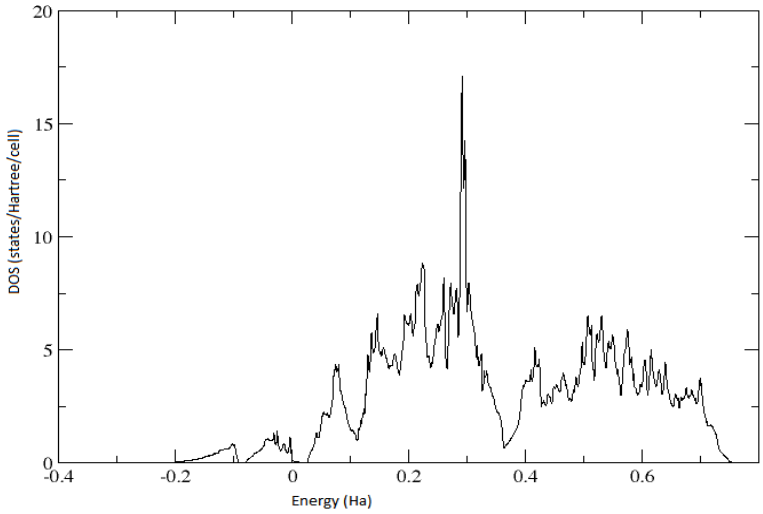

Figure 6: The P-3p orbital contribution to the DOS.

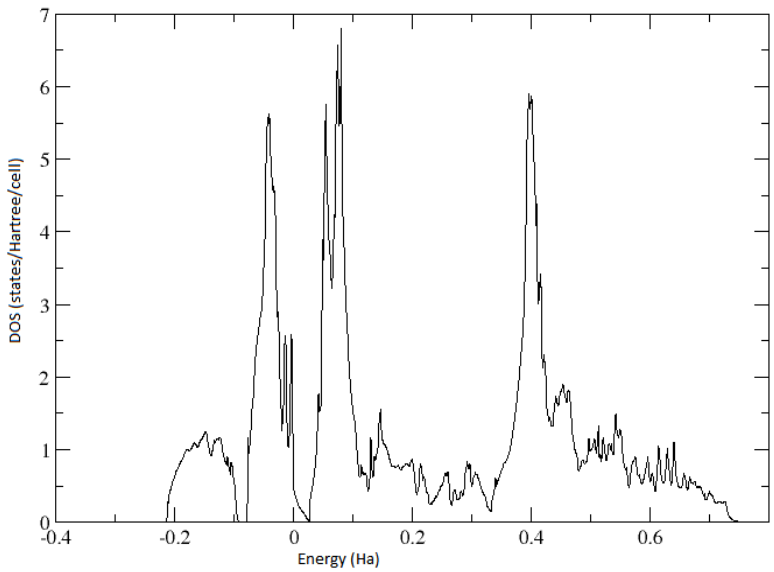

Figure 7: The Si-3s orbital contribution to the DOS.

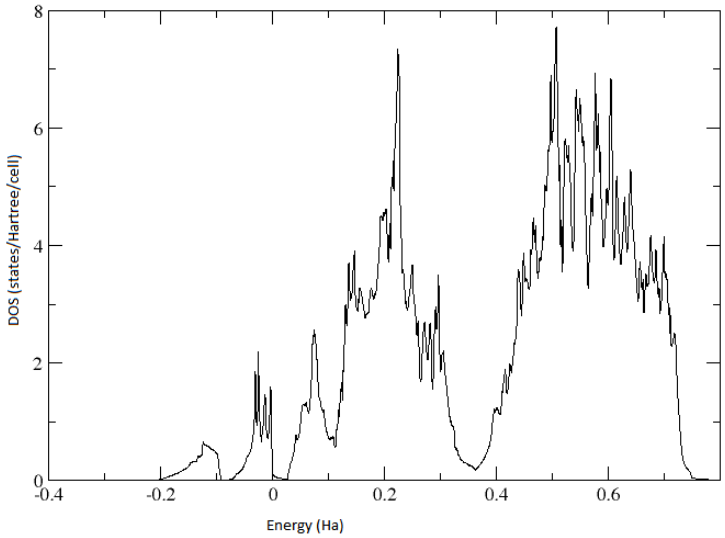

Figure 8: The Si-3p orbital contribution to the DOS.

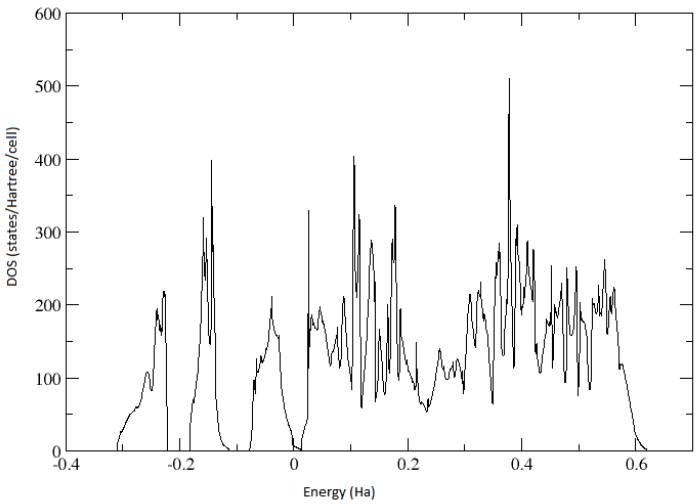

Figure 9: The total DOS for $SiAs_2$. The Fermi energy is at 0.24 Ha.

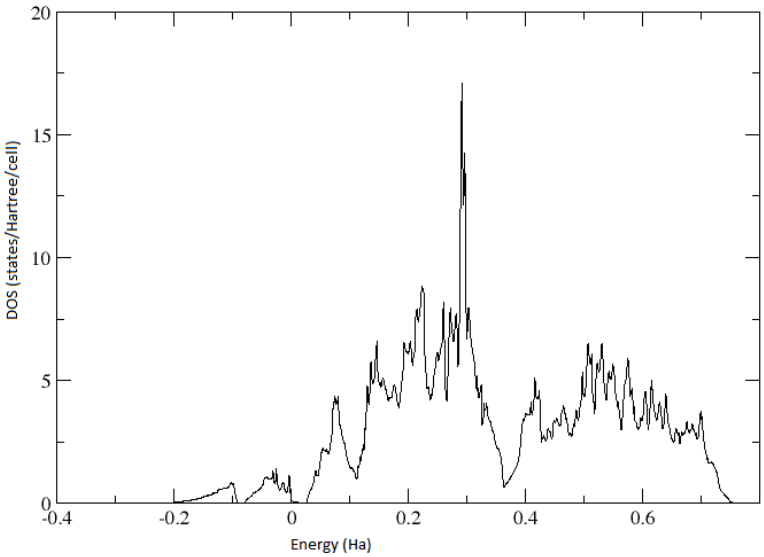

Figure 10: The P-3p orbital contribution to the DOS of $SiAs_2$.

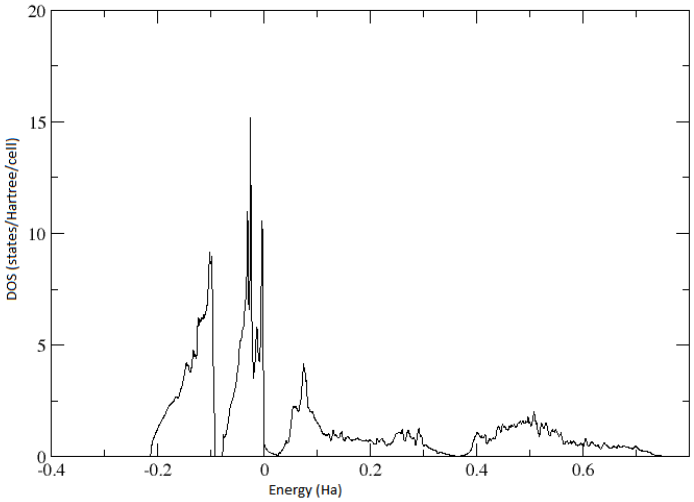

Figure 11: The P-3s orbital contribution to the DOS of $SiAs_2$.

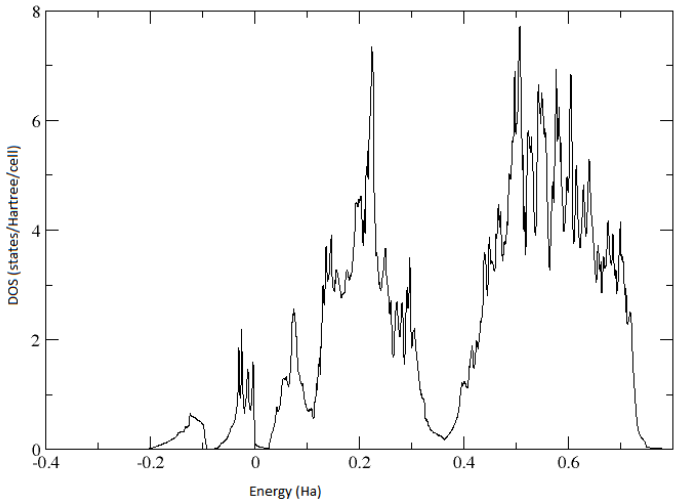

Figure 12: The Si-3p orbital contribution to the DOS of $SiAs_2$.

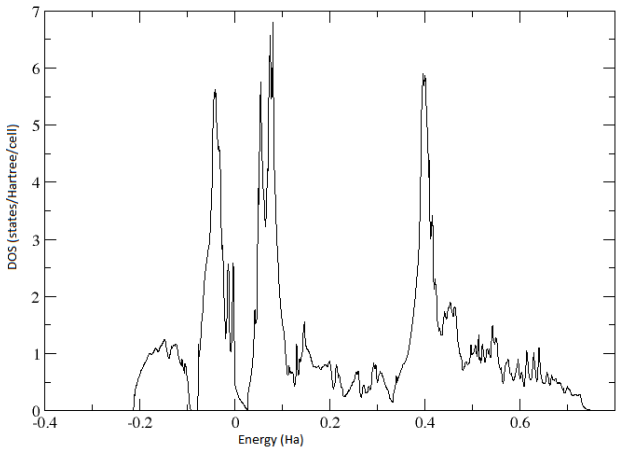

Figure 13: The Si-3s orbital contribution to the DOS of $SiAs_2$.

III. RESULTS AND DISCUSSION

The electronic band structure of SiP_2 and $SiAs_2$ plotted along lines of high symmetry in the first brilloun zone are shown in Fig. 2 and 3 respectively. In Fig. 2, the conduction band minimum (CBM) for the band structure of SiP_2 overlaps the Fermi energy level at the R high symmetry point with a negative band gap of -0.91 eV. This indicates that SiP_2 is semi-metallic in nature which agree well experimental results [1-6] and

previous theoretical investigation of Bachhuber et al. Also, the valence band maximum occurs at the X and gamma points of symmetry. Fig. 3 shows the electronic band structure of $SiAs_2$ also plotted along high symmetry points. Since SiP_2 is isomorphous with $SiAs_2$, the electronic band structure of SiP_2 is qualitatively the same. Except that the value of the band gap is -1.14 eV.

Fig. 4 shows the density of states (DOS) for SiP_2, and it reflects the semimetallic nature of the material as shown by the electronic band structure. The various orbital contribution to the DOS are shown in Fig. 5 to 8. It can be seen from Fig. 5 that the states within the energy range of -2 to 0 Ha are predominately the P-3s states. At the Fermi energy level however, there are no contribution from the P3s orbital. The states from 0 to 0.2 Ha, re made up of S-3s, Si-3p and P-3p orbitals as seen from Fig. 6 to 8. The states immediately below the Fermi energy level are composed of the P-3p and Si-3p orbitals. States across the Fermi energy level are mainly contributions from P-3p and Si-3p. The energy range from the Fermi level to about 0.4 Ha is predominately from the Si-3s orbital. Generally, all the orbital components seem to have significant contributions to the states in the conduction band except for P-3s.

Fig. 9 represents the DOS of $SiAs_2$. The Fermi energy level is at 0.24 Ha. The semi-metallic nature is well depicted by the DOS, which is in agreement with the electronic band structure. The orbital contribution to the DOS for $SiAs_2$ are shown in Fig. 10 to 13. The energy range of -0.2 to the 0 mark is dominated by the P-3s orbital, with significant contribution from S-3s coming in from about -0.1 to 0 Ha. States within the 0 to 0.24 Ha are mainly from P-3p and Si-3p, with a significant contribution from Si-3s from about 0 to 0.1 Ha. There is no significant contribution from the Si-3s and P-3s orbitals across the Fermi level. The states immediately above the Fermi level are predominately P-3p orbital while the energy range from 0.36 and beyond are Si-3p and P-3p dominated with a significant peak at about 0.41 Ha from the S-3s orbital.

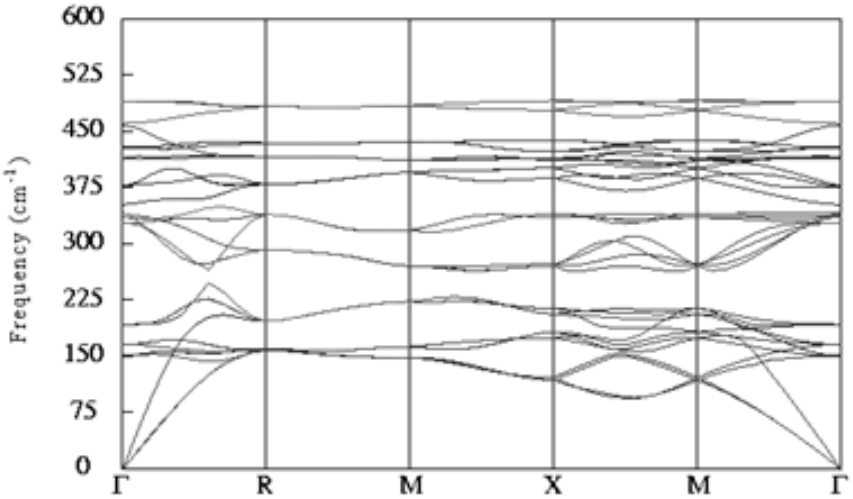

Figure 14: Phonon band structure of SiP_2.

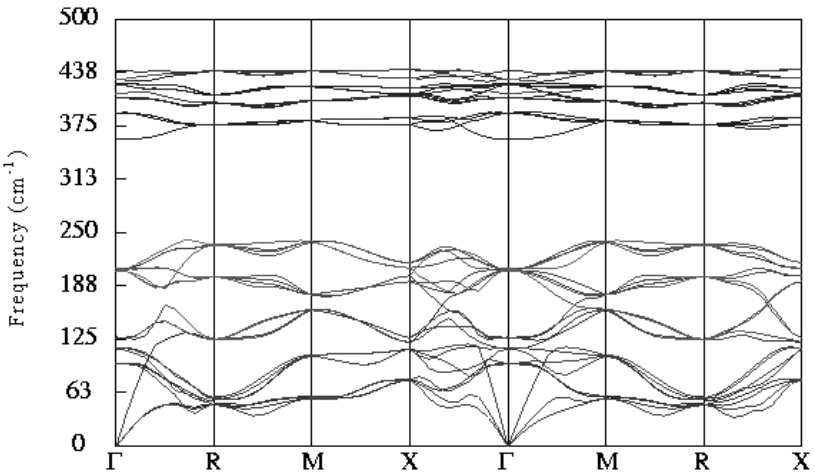

Figure 15: Phonon band structure of $SiAs_2$.

The phonon dispersion curves of $SiAs_2$and SiP_2along several high symmetry points in the brillouin (BZ) are displayed in Fig. 14 and 15 respectively. The unit cell is made up of four formula unit, that is, there are 12 atoms in the unit cell. There are a total of 36 frequency modes or bands, which are grouped into acoustic and optic modes. Three of the frequency modes are acoustic while the remainders are optic. In terms of the irreducible representations, the acoustic mode is given as $\Gamma_{acoustic} = T_u$ while $\Gamma_{optic} = A_g + 2A_u + E_g + 3E_u + 5T_u + 3T_g$ represents the optic modes. For the phonon curve of SiP_2 shown in figure 13, the analysis of degeneracies revealed that, of the (triply degenerate mode anti symmetric to inversion) $6T_u$ vibration modes, three are vibrations due to the Silicon atoms, while three are due to Phosphorus (P) atoms. The analysis also revealed that, the triply degenerate modes symmetric to inversion belonged to the P atoms with their corresponding frequencies as 323.7 cm^{-1}, 343.1 cm^{-1} and 487 cm^{-1} which are comparable to the experimental values of 319 cm^{-1}, 337 cm^{-1} and 485 cm^{-1}[8] respectively. The non-degenerate (single) mode of A_g and the doubly degenerate mode of E_g are attributed to the vibration of P atoms with values of 463.4 cm^{-1} and 360.3 cm^{-1} respectively. These agree well with the experimental values of 461 cm^{-1} and 353 cm^{-1} respectively. From figure 13, it can be seen that the phonon band structure is split into two with an energy window. This can have interesting property for the material, superconductivity is suggested. Also the bands with frequencies from 300 cm^{-1} and above are less disperse compared to bands with lower frequencies.

Fig. 15 shows the phonon band structure of $SiAs_2$ plotted along line of high symmetries. The analysis of degeneracies showed that, as in SiP_2, that of the (triply degenerate mode anti symmetric to inversion) $6T_u$ vibration modes, three are vibrations due to the Silicon atoms, while three are due to Arsenic (As) atoms. The $3T_g$ modes have their frequencies of vibrations as 442 cm^{-1}, 206 cm^{-1} and 205 cm^{-1} which are 45 cm^{-1}, 137.1 cm^{-1} and 118.7 cm^{-1} less than that corresponding to SiP_2. As in SiP_2, the dispersion curve is divided into two, leaving an energy window greater than that of SiP_2. The non-degenerate A_g mode and the doubly degenerate mode of E_g are attributed to the vibration of As atoms, and their values are 412 cm^{-1} and 208 cm^{-1} respectively. When compared to that of SiP_2, the E_g and A_g modes are about 52 cm^{-1} and 41 cm^{-1} less in $SiAs_2$ respectively.

IV. CONCLUSION

The electronic band structure and vibrational properties of SiP_2 and $SiAs_2$ have been calculated within the framework of the density functional theory (DFT) and the density perturbation functional theory (DPFT) respectively. For exchange and correlation, the local density approximation was used. The structural optimization results agree well with experiment. The calculation showed that both materials are semi-metals with negative band gap values of -0.91 eV and -1.14 eV for SiP_2 and $SiAs_2$ respectively. The highest frequency mode was observed to be one of the triply degenerated mode T_g with vibrational frequency value of 487 cm^{-1} for SiP_2 and 442 cm^{-1} for $SiAs_2$. The calculation also showed that, the phonon band structure is partitioned into two with a frequency interval. This interval is greater for $SiAs_2$. The calculated results for the various vibrational modes were found to be in excellent agreement with experiment results.

REFERENCES

[1]. Chattopadhyay T. K., and Schnering H. G. V., Pyrite-type silicon diphosphide p-SiP_2: structural parameter and valence electron density distribution, *Zeitschrift für kristallgraphie, 167,* 1984, 1-12.

[2]. Wadsten T., Synthesis of a Pyrite-Type Modification of SiP_2, *Acta Chem. Scand. 21, No 5,* 1967, 1374-1376.

[3]. Wadsten T., The crystal structure of SiAs, *Acta Chem. 19,* 1965, 1232-1238.

[4]. Pomerantseva E., Resini C., Kovnir K. and Kolenko Y. V., Emergingnanostructured electrode materials for water electrolysis and rechargeable beyond li-ion batteries, *Advances in Physics: X, 2;2,* 2017, 211-253. DOI:10.1080/23746149.2016.1273796.

[5]. Osugi J., Namikawa R. and Tanak Y., Chemical reaction at high temperature and high pressure, *the Review of Physical Chemistry of Japan, vol. 36, No. 1,* 1966, 35-43

[6]. Donohue P. C., Siemons W. J., Gillson J. L., Preparation and properties of pyrite-type SiP_2 and $SiAs_2$, *J. Phys. Chem. Solids 29,* 1968, 807-813.

[7]. Farberovich O. V., Domashevskaya E. P., Electron charge density in SiP_2 and $SiAs_2$, *Sov. Phys. –Semicond. 10,* 1976, 454-455.

[8]. Vogt H., Chattopadhyay T., Stolz H. J., Complete first-order Raman spectra of the pyrite structure compounds FeS_2, MnS_2 and SiP_2, *J. Chem. Solids 44,* 1983, 869-873.

[9]. Bachhuber F., Rothballer J., Pielnhofer F. and Weihrich R., First principle calculations on structure, bonding, and vibrational frequencies of SiP_2, *J. of Chem. Phys. 135,* 2011, 124508-7.

[10]. Bachelet G. W., Hamann D. R., and Schluter M., Pseudopotentials that work: from H to Pu, *Phys. Rev.* ***B*** *26,* 1982, 4199.

[11]. Gonze X., Beuken J.-M., Caracas R., Detraux F., Fuchs M., Rignanese G.-M., Sindic L., Verstraete M., Zerah G., Jollet F., Torrent M., Roy A., Mikami M., Ghosez Ph., Raty J.-Y., and Allan D.C., First-principles computation of material properties : the Abinit software project, *Computational Materials Science 25,* 2002, 478-492. (http://dx.doi.org/10.1016/S0927-0256(02)00325-7).

[12]. Gonze X., Rignanese G.-M., Verstraete M., Beuken J.-M., Pouillon Y., Caracas R., Jollet F., Torrent M., Zerah G., Mikami M., Ghosez Ph., Veithen M., Raty J.-Y., Olevano V., Bruneval F., Reining L., Godby R., Onida G., Hamann D. R., and Allan D. C., A brief Introduction to the Abinit software package. *Z. Kristallogr. 220,* 2005, 558-562.

[13]. Perdew J. P. and Zunger A., Self-interaction to density functional approximation for many-electron systems, *Phys. Rev B 23,* 1981, 5048-5079.

[14]. Gonze X., and Lee C., Dynamical matrices, Born effective charges, dielectric permittivity tensors, and interatomic forceconstants from density-functional perturbation theory**,** *Phys. Rev. B 55,* 1997, 10355-10368**.**

[15]. Lee C., and Gonze X., *Ab initio* calculation of the thermodynamic properties and atomic temperature factors of SiO2 α-quartz and stishovite, *Phys. Rev. B 51*, 1995, 8610-8613.
[16]. Baroni S., Gironcoli S, Corso A., and Giannozzi P., Phonons and related crystal properties from density-functional perturbation theory, *Rev. Mod. Phys. 73*, 2001, 515-562.
[17]. Wu P. and Huang M., Stability, bonding and electronic properties of Silicon and Germanium Arsenides, *Phys. Status Solidi B 253, No 5*, 2016, 862-867. DOI: 10.1002/PSSB.201552598.

Omehe N. N "Ab initio study of the electronic band structure and phonon dispersion spectra of Silicon disulphide (SiP2) and Silicon diarsenide (SiAs2).” American Journal of Engineering Research (AJER), vol. 6, no. 12, 2017, pp. 439-447.